SCIENTIFIC REPORTS
nature research

OPEN

Synthesis of nickel nanoparticles by a green and convenient method as a magnetic mirror with antibacterial activities

Mohammad Reza Ahghari, Vahhab Soltaninejad & Ali Maleki✉

In this work, a simple protocol was described for the synthesis of nickel magnetic mirror nanoparticles (NMMNPs) including antibacterial activities. The identification of NMNPs was carried out by field-emission scanning electron microscopy (FESEM) images, energy-dispersive X-ray (EDX) analysis, X-ray diffraction (XRD) pattern, transmission electron microscopy (TEM) images and vibrating sample magnetometer (VSM) curve. The antibacterial activities are investigated against *S. aureus* and *E. coli* as the Gram-positive and Gram-negative bacteria, respectively. The UV–Vis absorption was also studied in the present of NMMNPs at different time intervals that disclosed decreasing of the bacterial concentration. More than 80% of the bacteria were disappeared after treating in the presence of NMMNPs for 18 h. The Ni-NPs revealed an excellent mirror attribute with a well-controlled transmission (7%). A better light-reflectivity over conventional glass or a mercury mirror proved their utility for domestic uses in comparison with conventional mirrors as rather toxic materials like mercury. Owing to its magnetic properties, this kind of mirror can be easily made onto glass by using an external magnet. An ordered crystalline structure, admissible magnetic properties, substantial antibacterial activities, tunable mirror properties, mild reaction conditions, and overall, the facile synthesis are the specific features of the present protocol for the possible uses of NMMNPs in diverse applications.

Nanomaterials (NMs) in general render surface-controlled properties owing to a large surface-to-volume ratio, active energy carriers, and other variants useful for a variety of domestic uses[1–10]. Surface spins play a vital role in finely tuning magnetism and magnetic properties in magnetic nanoparticles (MNPs) of transition metals and other materials[11–16]. Several metals, such as Ag, Co, Ni, and Pd have been studied in the forms of NPs, with unique traits that promoted their usages in different applications[17–20]. Due, to remarkable properties like high reactivity, operational simplicity, biocompatibility, bacterial resistance, cost-effectiveness, abundance, anti-inflammatory activities, and environmental compatibilities, Ni-NPs attracted enormous interests and applied as a catalyst, an electro-catalyst, a photo-catalyst, a biosensor, and a heat-exchanger[21–40]. Many methods have been employed for the synthesis of Ni-NPs, namely, chemical reduction processes, discharge route, photocatalytic reduction, etc[41–44]. Most of these methods suffer from several disadvantages such as complex processing, complex reaction conditions, high temperatures, and long reaction times.

Synthesis of mirror films with NPs such as mercury, silver and gold has been reported in the various processes[45–47]. Most of the reported methods use toxic and expensive materials in which the mirror forms under challenging conditions. Significant characteristics of the mirror are its long-term durability and reflectivity, which are usually used in optical activities, wave-fronts, and solar cells[48–54]. It is an assembly of NPs that determines its reflectivity in the ultraviolet (UV)-visible regions of the electromagnetic spectrum[55,56]. Obviously, it is essential to prevent the risk of harmful bacteria in a public-health-safety. Therefore, various kinds of antibacterial agents are being developed. On the other hand, undesirable effects and consecutive of them lead to resistant to antibiotics. So, the synthesis of biocompatible antibacterial agents is one of the prime issues for scientists. The use of suitable NPs provides a high specific surface area and a high number density of active sites over the bulk values for these activities[6,57–61]. The metals like Ag, Ni, Zn, etc. are usefully reactive with proteins, and can stop

Catalysts and Organic Synthesis Research Laboratory, Department of Chemistry, Iran University of Science and Technology, Tehran 16846-13114, Iran. ✉email: maleki@iust.ac.ir

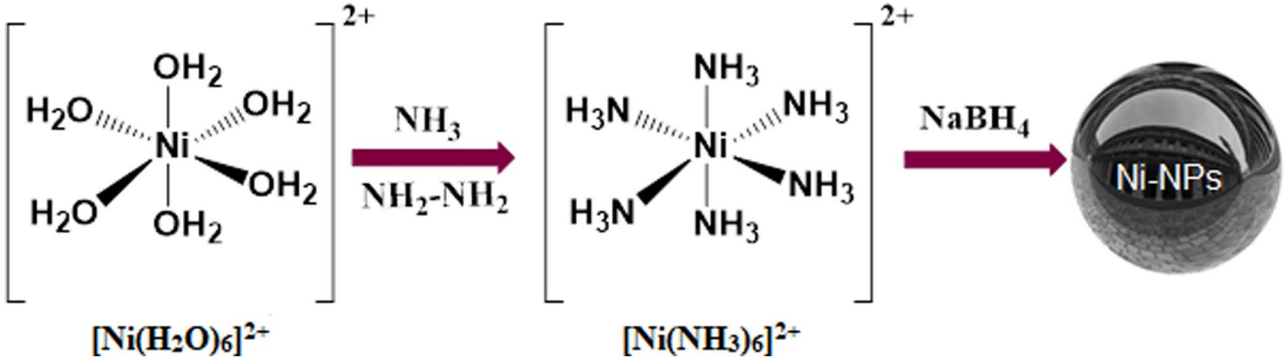

Figure 1. A schematic view of preparing NMMNPs in this work.

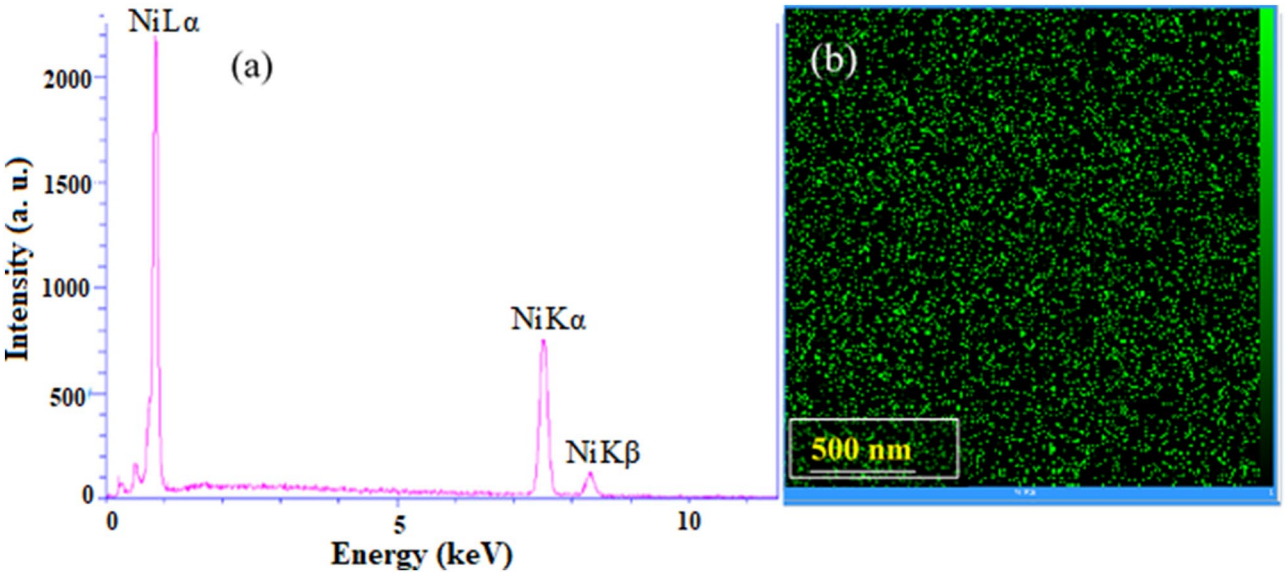

Figure 2. **(a)** EDX and **(b)** elemental mapping spectra of NMMNPs.

the regulated transport across the plasma membrane by permeability affecting the transport system and lead to the death of bacteria[62–65]. Some NMs, including Ag, Cu, or ZnO, act strongly against the vast species of bacterial and fungal[66–69]. Hence, the introduction of NMs with the features mentioned above by a green synthetic route is highly demanded. In this regard, due to the importance of mirrors in different industries like space telescopes, optoelectronics, and medicals, the design and synthesis of magnetic mirrors with fewer toxicity materials is highly appreciated[70–74]. Also, the mirrors with antibacterial properties are required in medical instruments. Therefore, in this work, nickel magnetic mirror nanoparticles (NMMNPs) are designed, synthesized and characterized via efficient procedures, showing excellent magnetic properties, antibacterial activities and diverse mirror properties (Fig. 1). The antibacterial activities are studied against *S. aureus*, a Gram-positive bacterium, and *E. coli*, a Gram-negative bacterium. The synergic properties of these NMMNPs can be used safely for various industrial applications.

Results and discussion

In this research, Ni-MNPs with mirror properties are synthesized for the first time by a simple method at ambient temperature in the water as an eco-friendly solvent. The synthesized NMMNs are characterized in terms of the FESEM/TEM images, XRD pattern, EDX spectrum, and magnetic properties. Ni retrievable MNPs are applied as a perfect mirror and the transmission is checked by their UV absorption spectra. Furthermore, acceptable antibacterial activities are studied by an agar disk diffusion and optical density (OD) analysis as follows.

Characterization of NMMNPs. An EDX analysis is performed to ensure the nickel content in the NMMNs. As can be seen in a typical EDX spectrum in Fig. 2a, a pure Ni is present in a single phase with a practically uniform distribution in the elemental mapping in Fig. 2b. The purity of the Ni-NPs was checked by ICP analysis, in which the Ni-NPs were dissolved in concentrated nitric acid and kept for 3 days to make a clear solution. Some residual boron (from $NaBH_4$ used in the reaction) was found below 10%. Figure 3a shows a rea-

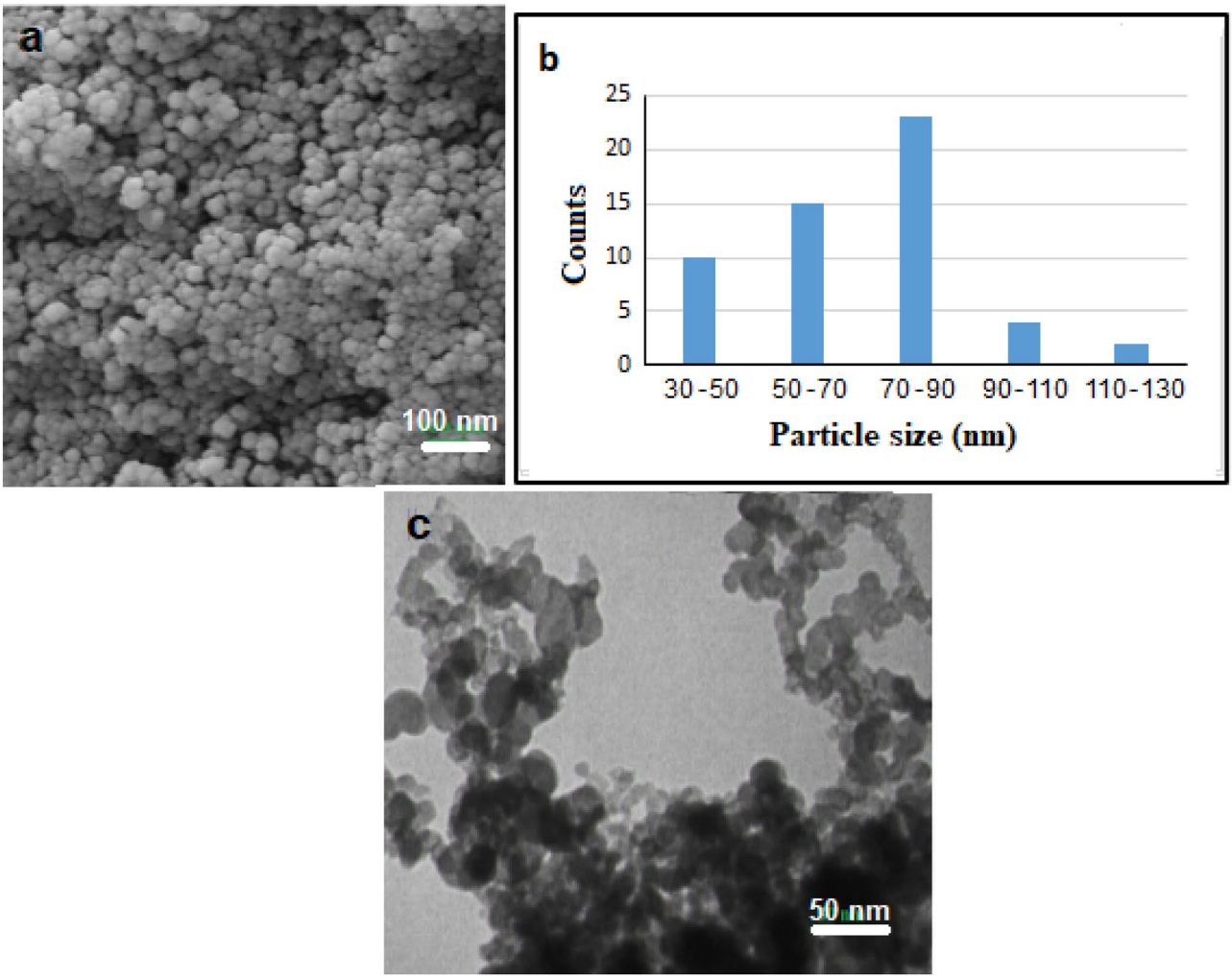

Figure 3. **(a)** FESEM images, **(b)** corresponding size distribution, and **(c)** TEM images of a sample of NMMNPs.

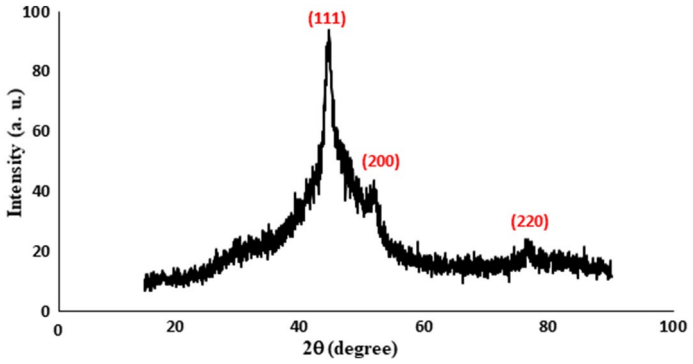

Figure 4. XRD pattern of a sample of NMMNPs.

sonably uniform distribution of FESEM images of NMMNs at a scale of 30 to 130 nm. Their size distributions are portrayed in a bar diagram in Fig. 3b in a majority of NPs have 50 to 90 sizes. A closer view of TEM images in Fig. 3c reveals mostly rectangular prisms of bit smaller sizes of the NMMNPs crystallites, mostly are varied in a 20 to 40 nm range. In fact, the small crystallites are arranged further in clusters of a hierarchical structure as observed in duly bigger sizes in the FESEM images in Fig. 3a.

Figure 4 shows the XRD pattern of three broad peaks of the sample of NMMNPs at diffraction angles 44.49°, 51.85° and 76.38° in the lattice reflections from the (111), (200), and (220) lattice planes, respectively, with an

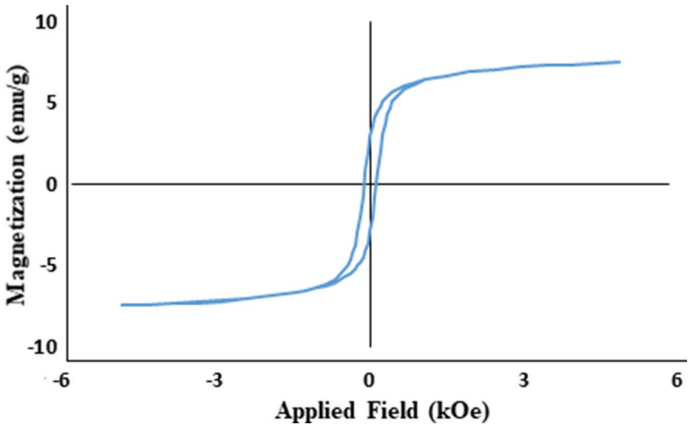

Figure 5. Magnetic hysteresis loop of a sample of NMMNPs.

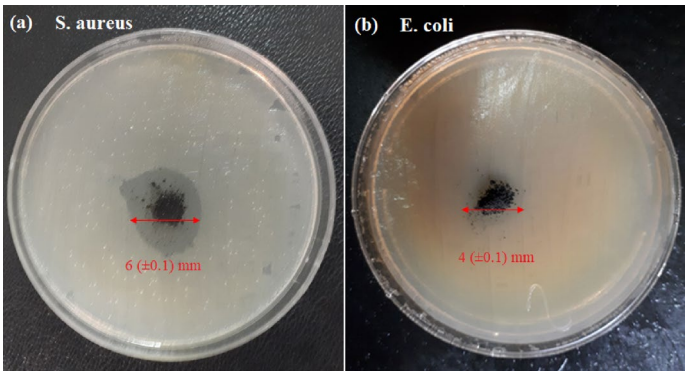

Figure 6. Agar disk diffusions of **(a)** *S. aureus* and **(b)** *E. coli* in the presence of NMMNPs.

average lattice parameter $a = 0.3522$ nm of a well-known fcc structure. A bit larger a-value is observed in comparison to a bulk fcc-Ni of $a = 0.3517$ nm of JCPDS card no. 01-087-0712. An average crystallite size D = 30 nm is calculated using the peak broadening in the Scherrer relation as described elsewhere[32,33].

A sample of NMMNPs exhibits a closed M-H hysteresis loop of magnetization (M) in Fig. 5 as measured in an applied magnetic field H of (-) 6 kOe to (+) 6 kOe at room temperature. The loop is well symmetrical of its shape over the field H, with a coercivity $H_c = 110$ Oe and an effectively lower saturation magnetization $M_s = 12$ emu/g, intrinsic of a soft ferromagnetic phase. A reduced $M_s = 12$ emu/g value (over a nearly 54.5 emu/g in a pure fcc-Ni)[23,26,27] observed here accounts in surface effects of the small crystallites of a cluster. A consistently small M_s is reported in Ni-NPs to form a soft magnetic mirror[42,76,77].

Antibacterial properties of NMMNPs. Figure 6 presents the digital images of Agar disk diffusions of (a) *S. aureus* and (b) *E. coli* in the presence of the NMMNPs developed in this work. As can be seen in the presence of 0.01 g Ni-NPs at 37 °C for 24 h, there is no any visible bacterial growth (zone) around 0.6 and 0.4 cm for *S. aureus* and *E. coli*, respectively, in the present experiments.

Further, we studied the OD measurements of bacterial cultures in the presence of 0.01 g Ni-NPs, 0.5 McFarland turbidity standard, and nutrient Broth media. The rate growth of bacterial was studied in 3, 6 and 18 h of stipulated time-intervals. As can be seen in a bar diagram in Fig. 7. The antibacterial activities show a noticeable inhibition of bacterial growth for *E. coli* compared to *S. aureus* after 6 h. However, only less than 22% of the bacteria remained viable after 18 h in both cases. The results confirm the effect of NMMNPs killing and inhibiting bacterial growth in terms of the UV absorption spectra in a SI file.

As usual, the colony counter method was applied to estimate the concentration of live bacteria in the cultured samples[78–82]. From the digital images given in Fig. 8, it is clear that the NMMNPs had inactivated the *E. coli* and *S. aureus* bacteria upon a critical 24 h of exposure. Similarly, the antibacterial performance of the Ni-NPs was evaluated in comparison to the results of the control obtained in the absence of the Ni-NPs under identical conditions.

Antimicrobial activities of NMMNPs. NMMNPs have antibacterial properties on *E. coli* and *S. aureus* in the bacterial plasma membrane is changed as comes in contact to Ni-NPs[78,79]. Cell death incurs by its permeability affecting its proper transport through the plasma membrane, leaving the bacterial cells incapable of

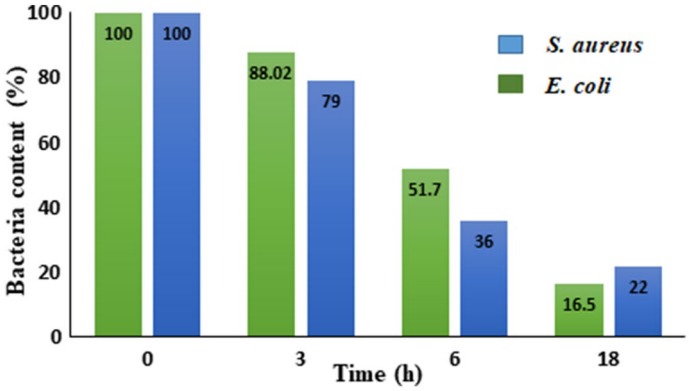

Figure 7. The OD diagram of *S. aureus* and *E. coli* in the presence of NMMNPs.

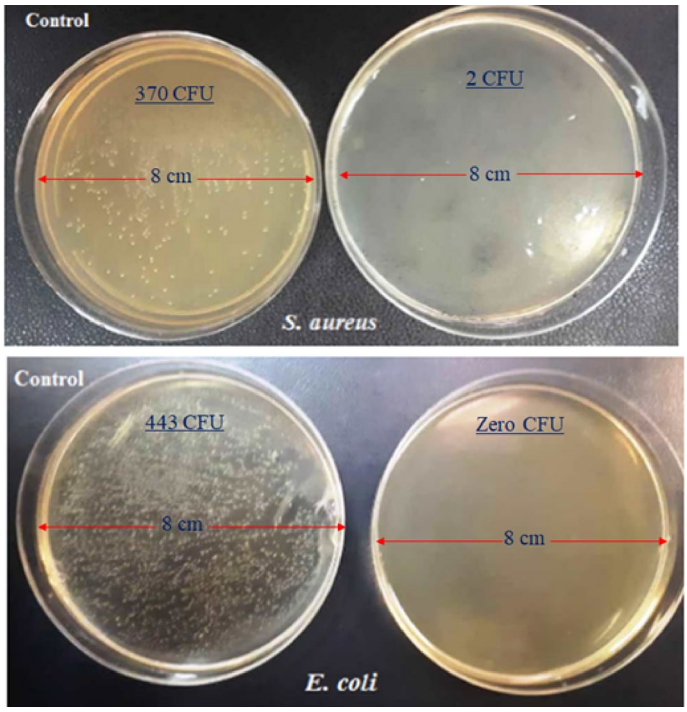

Figure 8. Images of *S. aureus* and *E. coli* in the absence and presence (in the right) of NMMNPs after 24 h of stipulated exposures.

properly regulating the due transport through the plasma membrane. Also, Ni-NPs have penetrated inside the bacteria and believed to damage them by interacting with phosphorous and sulfur containing compounds such as DNA. On exposed to selected bacterial, NMMNPs can release Ni ions and show the bactericidal efficiency[82,83].

Mirror properties of NMMNPs. The mirror property of the Ni-NPs is confirmed in terms of the fractional values of transmittance and reflectance of the sample. A wide UV–visible region of 300 to 800 nm was chosen for comparing the transmission values in the synthesized mirror and a reference glass. As shown in the spectra in Fig. 9, the two samples have the values of 7% and 70%, respectively. Evidently, Fig. 9a, the mirror passes only a small fraction of light in the UV–visible regions. Figure 9b, and glass transmits a lot of UV–visible regions.

Furthermore, the reflectance of NMMNPs was studied using a tungsten halogen lamp over in 340–850 nm range. A known intensity (I_1) of the light source was used to obtain the reflected values (I_2) from the mercury mirror, synthesized Ni-NPs, and a routine glass in terms of the reflectance spectra, as given in Fig. 10. Here, the mercury mirror displays a reasonably higher value than the glass and NMMNPs. A value of the reflectivity (%) = I_2/I_1 was estimated using the so obtained I_1 and I_2 values. As portrayed in Fig. 11, the mercury mirror has a better reflectance than the NMMNPs over an early 400–600 nm regime, while the NMMNPs resume a higher reflectance at the longer 700–800 nm wavelengths.

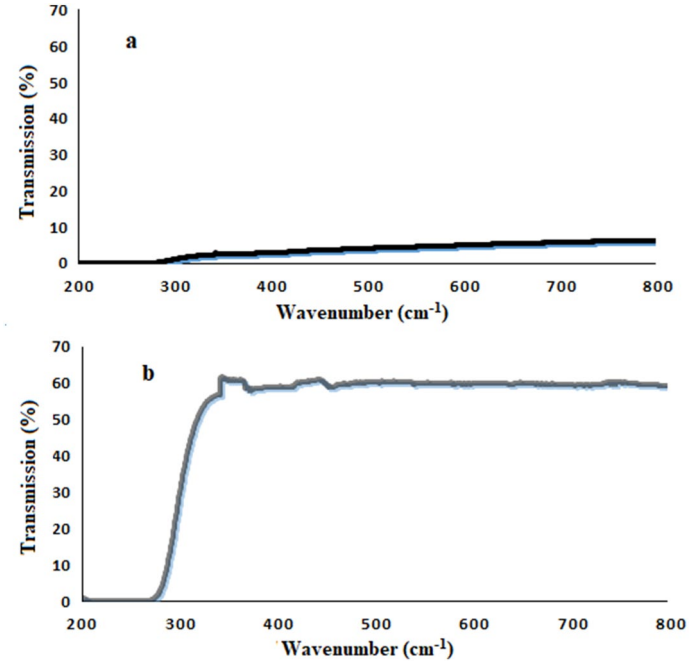

Figure 9. Transmittance spectra of **(a)** NMMNPs and **(b)** glass.

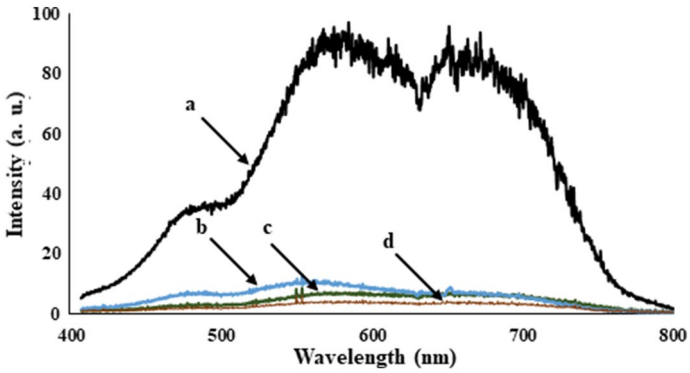

Figure 10. Intensity of light received to detector from **(a)** a tungsten halogen lamp, **(b)** a mercury mirror, **(c)** the synthesized NMMNPs, and **(d)** a routine glass.

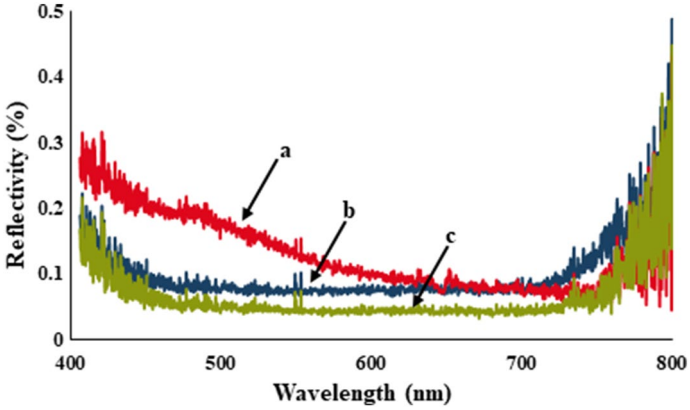

Figure 11. The reflectivity spectra of **(a)** a mercury mirror, **(b)** the synthesized NMMNPs, and **(c)** a routine glass.

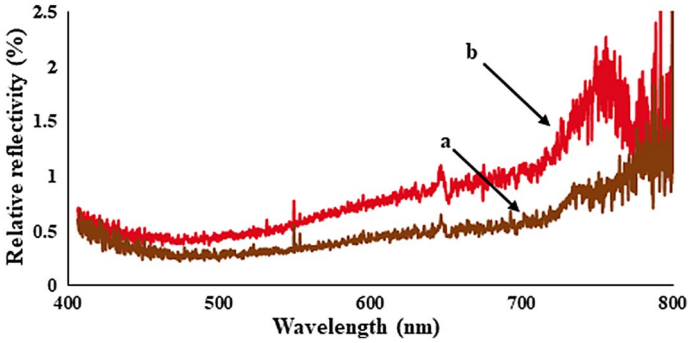

Figure 12. Reflectivity spectra of **(a)** glass and **(b)** NMMNPs over the mercury as a reference.

In general, the supremacy of the synthesized mirror of Ni-NPs can be visualized by expressing its relative reflectivity with respect to the mercury value. As this is portrayed in Fig. 12, the NMMNPs have quite acceptable value if compared to a routine glass what is it can be used as an alternative to the mirrors of toxic materials like mercury.

Experimental

Synthesis of NMMNPs. In a typical reaction batch, a 2 g of $NiCl_2{\cdot}6H_2O$ was taken in a 100 mL distilled water in a round-bottom flask to make a $[Ni(H_2O)_6]^{2+}$ complex. To form an aqueous complex $[Ni(NH_3)_6]^{2+}$, solutions of NH_3 and hydrazine hydrate (each of 20 mℓ) were added drop by drop to the green $NiCl_2{\cdot}6H_2O$ solution. The mixture was stirred for 2 h and then, a 0.20 g of $NaBH_4$ was added after the black solution resident stays for 48 h. The mirror was created on the internal surface of the bottom flask. Then, the extra solution was removed from the bottom, and the Ni-NPs were separated by an external magnet. To antibacterial tests and other analyses, the NMMNPs were washed repeatedly by distilled water and dried at 70 °C in an ambient atmosphere.

Structural analyses. The pure materials like metal salt, solvents and other chemicals were obtained from Sigma-Aldrich and Merck companies. The FESEM images were recorded by using a TESCAN VEGA3 microscope (with a provision to study EDX spectra from selected regions in conjunction with a Numerix DXP-X10P analyzer), while the TEM images were obtained by using a Philips CM120 instrument. The Bruker D8 advance was applied to measure the XRD patterns of the various samples. The magnetic properties were studied using a vibrating sample magnetometer (VSM) of Lakeshore 7407 (Meghnatis Kavir Kashan Co., Iran). A Shimadzu UV–visible Mini 1240 spectrophotometer was used to study the absorption spectra in the UV–visible region. The ICP analysis was provided on a Shimadzu ICPS-7000. An agar disk diffusion test was applied by agar plates that include an agar as a solid growth medium and nutrients microorganisms for antibacterial tests. Further, a 0.5 McFarland turbidity standard to Nutrient Broth media was applied for the antibacterial test. A tungsten halogen lamp was used to study the reflectance spectra in a 340–850 nm range.

Procedure of the antibacterial test. Gram-negative *Escherichia coli* and *Staphylococcus aureus* as Gram-positive bacteria were applied for antibacterial tests. A 0.01 g of NMMNPs was added to the agar plate containing bacteria. The Petri dishes were kept at 37 °C in an incubator for 24 h. All of the instruments have been sterilized at 121 °C. Further, the OD measurements were done by the addition of a 0.01 g of NMMNPs with 0.5 McFarland turbidity standard to Nutrient Broth media. The rate of bacterial killing was checked at various time-intervals in terms of the UV–visible spectra of the recovered samples. For the colony counter, a diluted 0.5 McFarland turbidity standard, a 0.1 g of Ni-NPs and a 0.2 mℓ of DMSO were added to nutrient Broth culture media. The mixture was kept at 37 °C in an incubator for 2 h. Then, a 0.1 mℓ of this mixture was kept in Mueller Hinton agar[78–83].

Conclusions

In summary, a simple, green, and efficient method has been introduced using a nickel-metal salt as a precursor for synthesizing Ni-NPs with useful features of the magnetic mirror, antibacterial activities and magnetic properties. The antibacterial activities of NMMNPs are studied for *S. aureus* and *E. coli bacteria* by a cup-plate agar diffusion method and OD measurements. The inactivated *E. coli* and *S. aureus* bacteria in the presence of NMMNPs were confirmed by colony method. The NMMNPs showed a marked sensitivity against *S. aureus* and *E. coli* in the *S. aureus* reveals a higher zone of inhibition than *E. coli* bacterium. An OD analysis verified that the killing and inhibiting bacterial growth is better than 80% in an 18 h exposure. The synthesized mirror has less than 7% transmission in a UV–visible light usefully for its possible applications. The NMMNPs are better reflective than a routine glass. Because of its low toxicity, a sample Ni-NPs can be used as an alternative to mirrors with toxic materials like Hg. Moreover, due to magnetic properties, a coating of NMMNPs on a glass as a highlight mirror feature of this report can be simply provided by an external magnet. As a result, in the reported properties and the synergistic effect of these features, the NMMNPs can be applied in domestic usages such as dentistry, surgery, laser tools, photonics, and space telescopes.

Received: 22 January 2020; Accepted: 16 July 2020
Published online: 28 July 2020

References

1. Zhao, H., Kang, X. & Liu, L. Comb–coil polymer brushes on the surface of silica nanoparticles. *Macromolecules* **38**, 10619–10622 (2005).
2. Wang, X. *et al.* Surface emission characteristics of ZnO nanoparticles. *Chem. Phys. Lett.* **423**, 361–365 (2006).
3. Faramarzi, M. A. & Forootanfar, H. Biosynthesis and characterization of gold nanoparticles produced by laccase from *Paraconiothyrium variabile*. *Colloids Surf. B* **87**, 23–27 (2011).
4. Kanmani, S. S. & Ramachandran, K. Synthesis and characterization of TiO2/ZnO core/shell nanomaterials for solar cell applications. *Renewable Energy* **43**, 149–156 (2012).
5. Gopalakrishnan, K., Ramesh, C., Ragunathan, V., Thamilselvan, M. Antibacterial activity of Cu_2O nanoparticles on *E. coli* synthesized from *Tridax procumbens* leaf extract and surface coating with polyaniline. *Dig. J. Nanomater. Biostruct.* **7**, 833–839 (2012).
6. Yang, Z. H., Zhuo, Y., Yuan, R. & Chai, Y. Q. An amplified electrochemical immunosensor based on in situ-produced 1-naphthol as electroactive substance and graphene oxide and Pt nanoparticles functionalized CeO_2 nanocomposites as signal enhancer. *Biosens. Bioelectron.* **69**, 321–327 (2015).
7. Kumar, S. G. & Rao, K. K. Tungsten-based nanomaterials (WO3 & Bi2WO6): Modifications related to charge carrier transfer mechanisms and photocatalytic applications. *Appl. Surf. Sci.* **355**, 939–958 (2015).
8. Hajizadeh, Z. & Maleki, A. Poly (ethylene imine)-modified magnetic halloysite nanotubes: A novel, efficient and recyclable catalyst for the synthesis of dihydropyrano[2,3-c]pyrazole derivatives. *Mol. Catal.* **460**, 87–93 (2018).
9. Bandala, E. R., Berli. M. Engineered nanomaterials (ENMs) and their role at the nexus of food, energy, and water. *Mater. Sci. Energy Technol.* **2**, 29–40 (2019).
10. Maleki, A., Hajizadeh, Z., Sharifi, V. & Emdadi, Z. A green, porous and eco-friendly magnetic geopolymer adsorbent for heavy metals removal from aqueous solutions. *J. Clean. Prod.* **215**, 1233–1245 (2019).
11. Ong, Q. K., Wei, A., Lin, X. M. Exchange bias in Fe/Fe_3O4 core-shell magnetic nanoparticles mediated by frozen interfacial spins. *Phys. Rev. B*, **80**, 134418, https://doi.org/10.1103/PhysRevB.80.134418 (2009).
12. Zhu, J. J., Yao, D. X., Zhang, S. C., Chang, K. Electrically controllable surface magnetism on the surface of topological insulators. *Phys. Rev. Lett.* **106**, 097201, https://doi.org/10.1103/PhysRevLett.106.097201 (2011).
13. Klein, N. D., Hurley, K. R., Feng, Z. V. & Haynes, C. L. Dark field transmission electron microscopy as a tool for identifying inorganic nanoparticles in biological matrices. *Anal. Chem.* **87**, 4356–4362 (2015).
14. Maleki, A., Hajizadeh, Z. & Firozi-Haji, R. Eco-friendly functionalization of magnetic halloysite nanotube with SO_3H for synthesis of dihydropyrimidinones. *Microporous Mesoporous Mater.* **259**, 46–53 (2018).
15. Maleki, A., Hajizadeh, Z. & Salehi, P. Mesoporous halloysite nanotubes modified by $CuFe_2O_4$ spinel ferrite nanoparticles and study of its application as a novel and efficient heterogeneous catalyst in the synthesis of pyrazolopyridine derivatives. *Sci. Rep.* **9**, 5552 (2019).
16. Taheri-Ledari, R. *et al.* High-performance sono/nano-catalytic system: Fe_3O_4@Pd/$CaCO_3$-DTT core/shell nanostructures, a suitable alternative for traditional reducing agents for antibodies. *Ultrason. Sonochem.* **61**, 104824 (2020).
17. Dastjerdi, R. & Montazer, M. A review on the application of inorganic nano-structured materials in the modification of textiles: Focus on anti-microbial properties. *Colloids Surf. B* **79**, 5–18 (2010).
18. Das, S. K. *et al.* Understanding the biosynthesis and catalytic activity of Pd, Pt, and Ag nanoparticles in hydrogenation and Suzuki coupling reactions at the nano–bio interface. *J. Phys. Chem. C* **118**, 24623–24632 (2014).
19. Yao, Y. *et al.* Fe Co, Ni nanocrystals encapsulated in nitrogen-doped carbon nanotubes as Fenton-like catalysts for organic pollutant removal. *J. Hazard. Mater.* **314**, 129–139 (2016).
20. Sharma, G., Kumar, A., Sharma, S., Naushad, M., Dwivedi, R. P., Alothman, Z. A., Mola, G. T. Novel development of nanoparticles to bimetallic nanoparticles and their composites: A review. *J. King Saud Univ.* **31**, 257–269 (2017).
21. Matsuo, T., Ueki, M., Takeyama, M. & Tanaka, R. Strengthening of nickel-base superalloys for nuclear heat exchanger application. *J. Mater. Sci.* **22**, 1901–1907 (1987).
22. Ram, S. & Frankwicz, P. S. Granular GMR sensors of Co–Cu and Co–Ag nanoparticles synthesized through a chemical route using $NaBH_4$. *Phys. Status Solidi A* **188**, 1129–1140 (2001).
23. Roy, A., Srinivas, V., Ram, S., De Toro, J. A. & Riveiro, J. M. Effect of interstitial oxygen on the crystal structure and magnetic properties of Ni nanoparticles. *J. Appl. Phys.* **96**, 6782–6788 (2004).
24. Conte, M., Prosini, P. P. & Passerini, S. Overview of energy/hydrogen storage: state-of-the-art of the technologies and prospects for nanomaterials. *Mater. Sci. Eng., B* **108**, 2–8 (2004).
25. Chen, J. *et al.* Optical properties of Pd–Ag and Pt–Ag nanoboxes synthesized via galvanic replacement reactions. *Nano Lett.* **5**, 2058–2062 (2005).
26. Roy, A., Srinivas, V., Ram, S., De Toro, J. A. & Mizutani, U. Structure and magnetic properties of oxygen-stabilized tetragonal Ni nanoparticles prepared by borohydride reduction method. *Phys. Rev. B* **71**, 184443 (2005).
27. Roy, A., Srinivas, V., Ram, S., De Toro, J. A. & Goff, J. P. A comprehensive structural and magnetic study of Ni nanoparticles prepared by the borohydride reduction of $NiCl_2$ solution of different concentrations. *J. Appl. Phys.* **100**, 094307 (2006).
28. Hu, F., Li, Z., Tu, C. & Gao, M. Preparation of magnetite nanocrystals with surface reactive moieties by one-pot reaction. *J. Colloid Interface Sci.* **311**, 469–474 (2007).
29. Kallempudi, S. S. & Gurbuz, Y. A nanostructured-nickel based interdigitated capacitive transducer for biosensor applications. *Sensors Actuators B Chem.* **160**, 891–898 (2011).
30. Sun, J., Su, Y., Rao, S. & Yang, Y. Separation of lysozyme using superparamagnetic carboxymethyl chitosan nanoparticles. *J. Chromatogr. B* **879**, 2194–2200 (2011).
31. Malvindi, M. A. *et al.* SiO_2 nanoparticles biocompatibility and their potential for gene delivery and silencing. *Nanoscale* **4**, 486–495 (2012).
32. Vaseem, M., Tripathy, N., Khang, G. & Hahn, Y. B. Green chemistry of glucose-capped ferromagnetic hcp-nickel nanoparticles and their reduced toxicity. *RSC Adv.* **3**, 9698–9704 (2013).
33. Singh, V., Ram, S. & Srinivas, V. Ferromagnetic nickel filled in borate shell by controlled oxidation–crystallization of boride in air. *J. Alloy. Compd.* **610**, 100–106 (2014).
34. Simonin, M. Richaume, a impact of engineered nanoparticles on the activity, abundance, and diversity of soil microbial communities: A review. *Environ. Sci. Pollut. Res.* **22**, 13710–13723 (2015).
35. Nagajyothi, P. C. *et al.* Antioxidant and anti-inflammatory activities of zinc oxide nanoparticles synthesized using *Polygala tenuifolia* root extract. *J. Photochem. Photobiol. B* **146**, 10–17 (2015).
36. Gong, M., Wang, D. Y., Chen, C. C., Hwang, B. J. & Dai, H. A mini review on nickel-based electrocatalysts for alkaline hydrogen evolution reaction. *Nano Res.* **9**, 28–46 (2016).

37. Bibi, I. *et al.* Nickel nanoparticle synthesis using *Camellia sinensis* as reducing and capping agent: Growth mechanism and photocatalytic activity evaluation. *Int. J. Biol. Macromol.* **103**, 783–790 (2017).
38. Seo, S., Perez, G. A., Tewari, K., Comas, X. & Kim, M. Catalytic activity of nickel nanoparticles stabilized by adsorbing polymers for enhanced carbon sequestration. *Sci. Rep.* **8**, 11786 (2018).
39. Jouyandeh, M. *et al.* Surface engineering of nanoparticles with macromolecules for epoxy curing: Development of super-reactive nitrogen-rich nanosilica through surface chemistry manipulation. *Appl. Surf. Sci.* **447**, 152–164 (2018).
40. Panáček, A. *et al.* Bacterial resistance to silver nanoparticles and how to overcome it. *Nat. Nanotechnol.* **13**, 65–71 (2018).
41. Li, D. & Komarneni, S. Microwave-assisted polyol process for synthesis of Ni nanoparticles. *J. Am. Ceram. Soc.* **89**, 1510–1517 (2006).
42. Roselina, N. N., Azizan, A., Hyie, K. M., Jumahat, A. & Bakar, M. A. Effect of pH on formation of nickel nanostructures through chemical reduction method. *Proc. Eng.* **68**, 43–48 (2013).
43. Muntean, A., Wagner, M., Meyer, J., Seipenbusch, M. Generation of copper, nickel, and CuNi alloy nanoparticles by spark discharge. *J. Nanoparticle Res. 18*, 229; https://doi.org/10.1007/s11051-016-3547-2 (2016).
44. El-Khatib, A. M., Badawi, M. S., Roston, G. D., Moussa, R. M. & Mohamed, M. M. Structural and magnetic properties of nickel nanoparticles prepared by arc discharge method using an ultrasonic nebulizer. *J. Cluster Sci.* **29**, 1321–1327 (2018).
45. Hadsund, P. The tin-mercury mirror: Its manufacturing technique and deterioration processes. *Stud. Conserv.* **38**, 3–16 (1993).
46. Gingras, J., Déry, J. P., Yockell-Lelièvre, H., Borra, E. & Ritcey, A. M. Surface films of silver nanoparticles for new liquid mirrors. *Colloids Surf. A* **279**, 79–86 (2006).
47. Mubeen, S. *et al.* Plasmonic properties of gold nanoparticles separated from a gold mirror by an ultrathin oxide. *Nano Lett.* **12**, 2088–2094 (2012).
48. Roux, P., de Rosny, J., Tanter, M. & Fink, M. The Aharonov-Bohm effect revisited by an acoustic time-reversal mirror. *Phys. Rev. Lett.* **79**, 3170. https://doi.org/10.1103/PhysRevLett.79.3170 (1997).
49. Yu, D. & Yam, V. W. W. Hydrothermal-induced assembly of colloidal silver spheres into various nanoparticles on the basis of HTAB-modified silver mirror reaction. *J. Phys. Chem. B* **109**, 5497–5503 (2005).
50. Shen, L., Ji, J. & Shen, J. Silver mirror reaction as an approach to construct superhydrophobic surfaces with high reflectivity. *Langmuir* **24**, 9962–9965 (2008).
51. Moulin, E. *et al.* Thin-film silicon solar cells with integrated silver nanoparticles. *Thin Solid Films* **516**, 6813–6817 (2008).
52. Inbaraj, B. S., Wang, J. S., Lu, J. F., Siao, F. Y. & Chen, B. H. Adsorption of toxic mercury (II) by an extracellular biopolymer poly(γ-glutamic acid). *Biores. Technol.* **100**, 200–207 (2009).
53. Gupta, I., Duran, N., Rai, M. Nano-silver toxicity: Emerging concerns and consequences in human health. In *Nano-Antimicrobials Progress and Prospects* (ed. Ciof, N., Rai, M.) 525–542 (Springer, New York, 2011).
54. Xu, X., He, W., Wang, C., Wei, M. & Li, B. SiNx thickness dependence of spectral properties and durability of protected-silver mirrors. *Surf. Coat. Technol.* **324**, 175–181 (2017).
55. Ritcey, A. M. & Borra, E. Magnetically deformable liquid mirrors from surface films of silver nanoparticles. *ChemPhysChem* **11**, 981–986 (2010).
56. Sun, X., Dou, J., Xie, F., Li, Y. & Wei, M. One-step preparation of mirror-like NiS nanosheets on ITO for the efficient counter electrode of dye-sensitized solar cells. *Chem. Commun.* **50**, 9869–9871 (2014).
57. Rai, M., Yadav, A. & Gade, A. Silver nanoparticles as a new generation of antimicrobials. *Biotechnol. Adv.* **27**, 76–83 (2009).
58. Lin, J. J., Lin, W. C., Li, S. D., Lin, C. Y. & Hsu, S. H. Evaluation of the antibacterial activity and biocompatibility for silver nanoparticles immobilized on nano silicate platelets. *ACS Appl. Mater. Interfaces.* **5**, 433–443 (2013).
59. Le Ouay, B. & Stellacci, F. Antibacterial activity of silver nanoparticles: A surface science insight. *Nano Today* **10**, 339–354 (2015).
60. Huo, P. *et al.* Fabricated Ag/Ag2S/reduced graphene oxide composite photocatalysts for enhancing visible light photocatalytic and antibacterial activity. *J. Ind. Eng. Chem.* **57**, 125–133 (2018).
61. Dadi, R., Azouani, R., Traore, M., Mielcarek, C., Kanaev, A. Antibacterial activity of ZnO and CuO nanoparticles against gram positive and gram negative strains. *Mater. Sci. Eng. C* **104**, 109968, https://doi.org/10.1016/j.msec.2019.109968 (2019).
62. El Ghandoor, H., Zidan, H. M., Khalil, M. M. & Ismail, M. I. M. Synthesis and some physical properties of magnetite (Fe_3O_4) nanoparticles. *Int. J. Electrochem. Sci.* **7**, 5734–5745 (2012).
63. Obaidat, I. M. *et al.* Investigating exchange bias and coercivity in Fe_3O_4–γ-Fe_2O_3 core–shell nanoparticles of fixed core diameter and variable shell thicknesses. *Nanomaterials* **7**, 415 (2017).
64. Chaudhary, J., Tailor, G., Yadav, B. L. & Michael, O. Synthesis and biological function of nickel and copper nanoparticles. *Heliyon* **5**, 2405–8440 (2019).
65. Park, S. B. *et al.* Silver-coated magnetic nanocomposites induced growth inhibition and protein changes in foodborne bacteria. *Sci. Rep.* **9**, 1–11 (2019).
66. Stanić, V. *et al.* Synthesis, characterization and antimicrobial activity of copper and zinc-doped hydroxyapatite nanopowders. *Appl. Surf. Sci.* **256**, 6083–6089 (2010).
67. Raghupathi, K. R., Koodali, R. T. & Manna, A. C. Size-dependent bacterial growth inhibition and mechanism of antibacterial activity of zinc oxide nanoparticles. *Langmuir* **27**, 4020–4028 (2011).
68. Samanovic, M. I., Ding, C., Thiele, D. J. & Darwin, K. H. Copper in microbial pathogenesis: Meddling with the metal. *Cell Host Microbe* **11**, 106–115 (2012).
69. Salem, W. *et al.* Antibacterial activity of silver and zinc nanoparticles against vibrio cholerae and enterotoxic *Escherichia coli*. *Int. J. Med. Microbiol.* **305**, 85–95 (2015).
70. Buser, R. A., De Rooij, N. F., Tischhauser, H., Dommann, A. & Staufert, G. Biaxial scanning mirror activated by bimorph structures for medical applications. *Sens. Actuators A* **31**, 29–34 (1992).
71. Vassiliev, V., Fegan, S. & Brousseau, P. Wide field aplanatic two-mirror telescopes for ground-based γ-ray astronomy. *Astropart. Phys.* **28**, 10–27 (2007).
72. Argueta-Figueroa, L., Morales-Luckie, R. A., Scougall-Vilchis, R. J. & Olea-Mejía, O. F. Synthesis, characterization and antibacterial activity of copper, nickel and bimetallic Cu–Ni nanoparticles for potential use in dental materials. *Prog. Nat. Sci.* **24**, 321–328 (2014).
73. Gahlawat, G. & Choudhury, A. R. A review on the biosynthesis of metal and metal salt nanoparticles by microbes. *RSC Adv.* **9**, 12944–12967 (2019).
74. Huang, Q. *et al.* Highly smooth, stable and reflective Ag-paper electrode enabled by silver mirror reaction for organic optoelectronics. *Chem. Eng. J.* **370**, 1048–1056 (2019).
75. Zhou, Y. H. & Zheng, X. A general expression of magnetic force for soft ferromagnetic plates in complex magnetic fields. *Int. J. Eng. Sci.* **35**, 1405–1417 (1997).
76. Barakat, N. A. *et al.* CoNi bimetallic nanofibers by electrospinning: Nickel-based soft magnetic material with improved magnetic properties. *J. Phys. Chem. C* **114**, 15589–15593 (2010).
77. Rausch, P., Verpoort, S. & Wittrock, U. Unimorph deformable mirror for space telescopes: Environmental testing. *Opt. Express* **24**, 1528–1542 (2016).
78. Saghatforoush, L. A., Mehdizadeh, R. & Chalabian, F. Hydrothermal and sonochemical synthesis of a nano-sized nickel (II) Schiff base complex as a precursor for nano-sized nickel (II) oxide; Spectroscopic, catalytic and antibacterial properties. *Transit. Met. Chem.* **35**, 903–910 (2010).

79. Pang, H., Lu, Q., Chen, C., Liu, X. & Gao, F. Facile synthesis of $Ni_3(BO_3)_2$ nanoribbons and their antimicrobial, electrochemical and electrical properties. *J. Mater. Chem.* **21**, 13889–13894 (2011).
80. Haldorai, Y. & Shim, J. J. Chitosan-zinc oxide hybrid composite for enhanced dye degradation and antibacterial activity. *Compos. Interfaces* **20**, 365–377 (2013).
81. Das, D., Nath, B. C., Phukon, P. & Dolui, S. K. Synthesis and evaluation of antioxidant and antibacterial behavior of CuO nanoparticles. *Colloids Surf. B* **101**, 430–433 (2013).
82. Shamaila, S. *et al.* Antibacterial effects of laser ablated Ni nanoparticles. *Appl. Phys. Lett.* **103**, 153701 (2013).
83. Chaudhary, R. G., Tanna, J. A., Gandhare, N. V., Rai, A. R. & Juneja, H. D. Synthesis of nickel nanoparticles: microscopic investigation, an efficient catalyst and effective antibacterial activity. *Adv. Mater. Lett.* **6**, 990–998 (2015).

Acknowledgements
The authors gratefully acknowledge the partial support from the Research Council of the Iran University of Science and Technology.

Authors contributions
A.M. has designed the study and managed the project. M.R.A. carried out the analyses, characterization and participated in discussing the results. V.S. prepared the draft of the manuscript and revised the manuscript. All authors read and approved the final manuscript.

Competing interests
The authors declare no competing interests.

Additional information
Supplementary information is available for this paper at https://doi.org/10.1038/s41598-020-69679-4.

Correspondence and requests for materials should be addressed to A.M.

Reprints and permissions information is available at www.nature.com/reprints.

Publisher's note Springer Nature remains neutral with regard to jurisdictional claims in published maps and institutional affiliations.